Journal of Neurochemistry

JOURNAL OF NEUROCHEMISTRY | 2011 | 119 | 826–838

doi: 10.1111/j.1471-4159.2011.07462.x

ORIGINAL ARTICLE

Amyotrophic lateral sclerosis-immunoglobulins selectively interact with neuromuscular junctions expressing P/Q-type calcium channels

Laura E. Gonzalez,*,† Mónica L. Kotler,† Lucas G. Vattino,* Eugenia Conti,‡ Ricardo C. Reisin,‡ Kirk J. Mulatz,§ Terrance P. Snutch§ and Osvaldo D. Uchitel*

*Departamento de Fisiología, Biología Molecular y Celular, Facultad de Ciencias Exactas y Naturales, IFIBYNE-CONICET, UBA, Argentina

†Departamento de Química Biológica, Facultad de Ciencias Exactas y Naturales, UBA, Argentina

‡Servicio de Neurología, Hospital Británico, Argentina

§Michael Smith Laboratories, University of British Columbia, Vancouver, Canada

Abstract

Amyotrophic lateral sclerosis (ALS) is a fatal neurodegenerative disease characterized by a gradual loss of motoneurons. The majority of ALS cases are associated with a sporadic form whose etiology is unknown. Several pieces of evidence favor autoimmunity as a potential contributor to sporadic ALS pathology. To gain understanding concerning possible antigens interacting with IgGs from sporadic ALS patients (ALS–IgGs), we studied immunoreactivity against neuromuscular junction (NMJ), spinal cord and cerebellum of mice with and without the $Ca_V2.1$ pore-forming subunit of the P/Q-type voltage-gated calcium (Ca^{2+}) channel. ALS–IgGs showed a strong reactivity against NMJs of wild-type diaphragms. ALS–IgGs also increased muscle miniature end-plate potential frequency, suggesting a functional role for ALS–IgGs on synaptic signaling. In support, in mice lacking the $Ca_V2.1$ subunit ALS–IgGs showed significantly reduced NMJ immunoreactivity and did not alter spontaneous acetylcholine release. This difference in reactivity was absent when comparing N-type Ca^{2+} channel wild-type or null mice. These results are particularly relevant because motoneurons are known to be early pathogenic targets in ALS. Our findings add further evidence supporting autoimmunity as one of the possible mechanisms contributing to ALS pathology. They also suggest that serum autoantibodies in a subset of ALS patients would interact with NMJ proteins down-regulated when P/Q-type channels are absent.

Keywords: amyotrophic lateral sclerosis, autoantibodies, autoimmunity, calcium channels.

J. Neurochem. (2011) **119**, 826–838.

Amyotrophic lateral sclerosis (ALS) is a neurodegenerative disorder characterized by progressive neuromuscular dysfunction and decrease in the number of upper and lower motoneurons (Mulder 1982). Clinical manifestations include fatigue, fasciculations, spasticity, hyperreflexia, weakness and muscle atrophy, ultimately leading to paralysis and death (Rowland 1998). Currently, there are no effective treatments to either stop or delay ALS progression.

Approximately 10% of patients present a familiar form of the disorder (fALS) characterized molecularly by underlying mutations in several different genes (Valdmanis *et al.* 2009). The remaining ALS cases (~90%) are sporadic (sALS) and of unknown etiology. Different hypotheses have been

Received June 11, 2011; revised manuscript received August 25, 2011; accepted August 25, 2011.

Address correspondence and reprint requests to Osvaldo D. Uchitel, Laboratorio de Fisiología y Biología Molecular, Facultad de Ciencias Exactas y Naturales, Universidad de Buenos Aires, Ciudad Universitaria, pabellón 2, piso 2, C1428EHA, Ciudad Autónoma de Buenos Aires, Argentina. E-mail: odu@fbmc.fcen.uba.ar

Abbreviations used: ALS, amyotrophic lateral sclerosis; ANOVA, analysis of variance; BSA, bovine serum albumin; Ca^{2+}, calcium; DC, disease control; DMEM, Dulbecco's modified Eagle's medium; fALS, familiar ALS; HC, healthy control; HCl, chlorhydric acid; HEK, human embryonic kidney; MEPP, miniature end-plate potential; NMJ, neuromuscular junction; PBS, phosphate-buffered saline; RN, Ringer's normal solution; sALS, sporadic ALS; SDS, sodium dodecylsulfate; TMR, tetramethylrhodamine; WT, wild-type.

proposed to explain sALS pathogenesis, including antibody-mediated autoimmunity (Appel *et al.* 1993; Pagani *et al.* 2006), glutamate excitotoxicity (Rothstein *et al.* 1992; Van Den Bosch *et al.* 2006), oxidative damage (Bowling *et al.* 1993; Niebroj-Dobosz *et al.* 2004) and neurofilament aggregation (Xu *et al.* 1993; Mendonca *et al.* 2005). There is considerable evidence supporting immune-mediated mechanisms in motoneuronal degeneration. First, autoimmune disorders have been demonstrated in ALS patients (Appel *et al.* 1986) along with serum antibodies against gangliosides (Pestronk *et al.* 1989), neurofilaments (Couratier *et al.* 1998) and voltage-dependent calcium (Ca^{2+}) channels (Smith *et al.* 1992). Secondly, spinal inflammatory infiltrates have been detected in ALS patients (Engelhardt and Appel 1990; Troost *et al.* 1990), as well as IgGs in endoplasmic reticulum of spinal and cortical motoneurons (Engelhardt and Appel 1990). However, the presence and pathophysiological relevance of autoantibodies remains controversial (Drachman and Kuncl 1989; Drachman *et al.* 1995; Arsac *et al.* 1996).

In guinea pigs' spinal cords, upper and lower motoneuron injury was observed when they were inoculated with bovine spinal homogenates (Engelhardt *et al.* 1990; Xu *et al.* 2009), resembling human ALS with regard to the presence of IgGs within motoneurons and inflammatory cells (Appel *et al.* 1991). Additionally, passive transfer of IgGs from immunized animals (Appel *et al.* 1991) or ALS patients (Uchitel *et al.* 1992b) can induce neuromuscular dysfunction in injected mice. In the latter instance, human IgGs were subsequently detected at motoneuronal soma and nerve terminals (Fratantoni *et al.* 1996; Engelhardt *et al.* 2005).

In vitro studies have shown that ALS–IgGs can induce apoptosis in spinal cord cultures and motoneuron cell lines, presumably by increasing intracellular Ca^{2+} concentration (Smith *et al*. 1994; Demestre *et al.* 2005). At neuromuscular junctions (NMJs), pre-incubation with ALS–IgGs stimulates spontaneous and asynchronous synaptic activity (Uchitel *et al.* 1988, 1992b; Pagani *et al.* 2006), Ca^{2+} influx (Mosier *et al.* 1995) and signaling pathways leading to Ca^{2+} release from intracellular stores (Pagani *et al.* 2006).

In all of these processes, an involvement of NMJ Ca^{2+} channels has been established. At NMJs evoked-transmitter release in response to Ca^{2+} influx is mediated mainly by P/Q-type Ca^{2+} channels (encoded by the $Ca_V2.1$ subunit; Protti *et al.* 1991; Starr *et al.* 1991; Uchitel *et al.* 1992a; Stea *et al.* 1994; Katz *et al.* 1997). Furthermore, the presence of L-type channels at motor end-plates (Urbano and Uchitel 1999) has been attributed to modulation of fast acetylcholine vesicle recycling (Perissinotti *et al.* 2008). Finally, N-type Ca^{2+} activity is critical for synaptic transmission early during development and in $Ca_V2.1$-lacking animals (Rosato Siri and Uchitel 1999; Urbano *et al.* 2003).

Given the proposed interaction between ALS–IgGs and Ca^{2+} channels (Llinas *et al.* 1993; Smith *et al.* 1994; Carter and Mynlieff 2003; Pagani *et al.* 2006), we evaluated the IgG reactivity effects in mouse models of genetic deletion of the $Ca_V2.1$ (P/Q-type; Bourinet *et al.* 1999) and $Ca_V2.2$ (N-type; Dubel *et al.* 1992) subunits. Our results suggest that NMJ antigens recognized by ALS–IgGs require the presence of P/Q-type channels, although the $Ca_V2.1$ subunit itself does not seem to be the major antigen.

Materials and methods

Animal genotyping

Determination of mice genotype was performed by multiplex PCR using mice tail biopsies. DNA samples were purified with DNeasy Tissue Kit (Qiagen Inc., Valencia, CA, USA) after tissue digestion with proteinase K (2 mg/mL) for 15 h at 56°C. Primers used for genotyping were:

$Ca_V2.1$ forward: 5′-CCAGCTTGAGTGGCCGCAGCACACG-3′
$Ca_V2.1^{+/+}$ reverse: 5′-ATAATAAGTCACCTCTGGTTCTAAAG-3′
$Ca_V2.1^{-/-}$ reverse: 5′-CTGACTAGGGGAGGAGTAGAAG-3′
$Ca_V2.2$ forward: 5′-TGGCACCTTATGCCTTGCACGGTGCCTGCG-3′
$Ca_V2.2^{+/+}$ reverse: 5′-GGTCGAGATGGCTTGCGGGACCCGTTGGGA-3′
$Ca_V2.2^{-/-}$ reverse: 5′-GCCTGCTTGCCGAATATCATGGTGGAAAAT-3′

The following amplification protocol was used:

$Ca_V2.1$ genotyping:
95°C for 3 min
95°C for 30 s, 55°C for 30 s, 72°C for 30 s (35 cycles)
72°C for 5 min
$Ca_V2.2$ genotyping:
94°C for 2 min
94°C for 20 s, 58°C for 20 s, 72°C for 40 s (35 cycles)
72°C for 7 min

PCR products were subjected to electrophoresis in a 1% (wt/vol) agarose gel containing ethidium bromide and bands analyzed according to their expected size: 240 bp for $Ca_V2.1^{+/+}$, 390 bp for $Ca_V2.1^{-/-}$, 460 bp for $Ca_V2.2^{+/+}$ and 580 bp for $Ca_V2.2^{-/-}$.

Human serum samples

Patients were diagnosed with sporadic ALS according to El Escorial criteria (Brooks 1994). All participating individuals provided written consent to take part in the study and the applied protocol was approved by the Institutional Review Board of the Hospital Británico of Buenos Aires. Age at diagnosis ranged from 59 to 76 (mean: 64.6 years) and the sex ratio was 6 : 2 (M : F). Six patients had spinal onset while the rest showed bulbar onset. All of the clinical parameters evaluated in each ALS patient (ALS Functional Rating and Norris Scales) had similar values (Table 1). Exclusion of genetic forms of ALS was based upon family history.

Disease controls (DC; $n = 7$; 4 females; mean age: 56.0 years) comprised people with Lambert-Eaton myasthenic syndrome (an autoimmune disorder against voltage-dependent Ca^{2+} channels, DC1), myasthenia gravis (an autoimmune disease against acetylcholine receptors, DC2), Charcot-Marie-Tooth (a purely genetic motoneuron disease involving myelin sheath destruction, DC3), fALS (DC4-6) and multifocal motor neuropathy with conduction block (an autoimmune disease against myelin sheath, DC7).

Table 1 Clinical parameters of sporadic ALS patients

Patient	Age (years)	Sex	ALS	VFC	Scores		Progression time (months)
					ALSFR[a]	Norris[b]	
ALS1	66	M	Definite	Abnormal	22	49	4
ALS2	70	F	Definite	Normal	NA	NA	12
ALS3	67	M	Definite	Normal	33	68	12
ALS4	62	M	Probable	Abnormal	32	38	18
ALS5	70	F	Definite	Normal	30	73	30
ALS6	77	M	Possible	Abnormal	35	71	60
ALS7	59	M	Definite	Normal	27	80	18
ALS8	67	M	Definite	Normal	28	59	24

VFC, vital force capacity; ALSFR, ALS functional rating; M, male; F, female; NA, not available.
[a]ALSFR Score ranges from 0 (pathological) to 40 (normal).
[b]Norris Score ranges from 0 (pathological) to 99 (normal).

Healthy controls (HC) consisted of three subjects with no evidence of neurological diseases (two females, mean age: 36.7 years). Blood samples were collected at the time of clinical evaluation. Serum was separated by centrifugation and stored at −80°C until purification.

IgG purification

All of the procedure was performed at 4°C. Serum samples were centrifuged at 12 000 *g* for 10 min and the supernatant subjected to ammonium sulfate fractionation to a final salt concentration of 50% (wt/vol). The solution was stirred for 60 min and centrifuged at 12 000 *g* for 30 min. The resulting pellet was resuspended in phosphate buffer (20 mM pH 7.0) and dialyzed against the same solution for 16 h using a 12-kDa pore cellulose membrane. IgG isolation was performed by affinity chromatography employing a ProteinG-Agarose column and 20 mM phosphate buffer as washing buffer. IgGs were eluted with glycine (0.1 M pH 2.7) and then acid-neutralized with Tris–HCl (1.0 M pH 9.0). The isolated fractions were subsequently dialyzed against phosphate-buffered saline (PBS; 10 mM phosphate buffer, 150 mM NaCl, 3 mM KCl pH 7.4) for 5 h. IgG concentrations were estimated by absorbance analysis at 280 nm, taking into consideration the human IgG molar absorptivity coefficient. Testing of purified fractions was performed by electrophoresis in 10% (wt/vol) sodium dodecylsulfate (SDS)-polyacrylamide gels and subsequent staining with Coomassie blue. Aliquots were stored at −20°C.

Animal handling

Animals were treated in accordance with national guidelines for the humane treatment of laboratory animals from University of Buenos Aires, which are comparable to those of the USA National Institutes of Health. All possible efforts were made to reduce the number of animals used and any suffering/discomfort.

For all the experiments, tissue was extracted from three different mice strains: Swiss (males, P > 30), $Ca_V2.1$-null strain sv129 (males and females, P16-P23) and $Ca_V2.2$-null strain C57BL/6 (males, P18). Both null strains were kindly provided by Dr Shin Hee-Sup (Korea Institute of Science and Technology, Seoul, Republic of Korea).

Intracellular recordings

Mice were anesthetized with an intraperitoneal overdose of 2% (wt/vol) tribromoethanol (0.3 mL/10 g body weight), exsanguinated and killed by beheading. Diaphragm muscle dissections were carried out in a Sylgard-covered Petri dish (Dow Corning, Midland, MI, USA) containing Ringer's normal solution (RN; 137 mM NaCl, 5 mM KCl, 2 mM $CaCl_2$, 1 mM $MgSO_4$, 12 mM $NaHCO_3$, 1 mM Na_2HPO_4 and 11 mM glucose pH 7.2–7.4), continuously bubbled with 95% O_2/5% CO_2. All procedures were carried out at room temperature (20–23°C) except as otherwise stated.

Phrenic nerve-muscle preparations were dissected and placed in a 1 mL volume recording chamber and incubated for 4 h in a humidified atmosphere with purified IgGs from either ALS patients or control subjects. IgGs were diluted in RN to a final concentration of 0.4 mg/mL. Either the right or left hemi-diaphragm was randomly used to test immunoglobulins.

Miniature end-plate potentials (MEPP) frequency was determined in the absence of tetrodotoxin (spontaneous activity), before and after the incubation period, using intracellular recordings (glass microelectrodes filled with 3.0 M KCl, 20–30 MΩ). Recordings of 2–5 min duration were randomly acquired from a maximum of 15 fibers from a minimum of 3 mice. Acquisition procedures were performed as previously described (Pagani *et al.* 2006). Data were stored on disk for further computer analysis using appropriate software (Axoscope 9.0 and Clampfit 9.0, Axon Instruments, Foster City, CA, USA). SigmaPlot 10.0 integrated with SigmaStat 3.5 (Systat Software Inc., Chicago, IL, USA) was used to compare and plot the data.

Neuromuscular junction immunofluorescence

Diaphragm dissection was performed as described above. Dissected muscles were fixed at 4°C in 4% (wt/vol) paraformaldehyde, permeabilized with 1% (vol/vol) Triton-X-100 and cryopreserved in 30% (wt/vol) sucrose. Optimum cutting temperature 4583 Tissue-Tek (Sakura, Tokyo, Japan) was employed as inclusion medium to generate 40-μm thick sections in a cryostat (ETR2248, Reichert-Jung, Bensheim, Germany), which were then mounted on gelatin-coated slides and stored at −20°C. To reduce background signal from muscle fibers, diaphragms were tangentially sliced and consequently, NMJs rarely showed the usual pretzel-like shape.

Tissue preparations were permeabilized with Triton-X100 0.05% (vol/vol) and subsequently blocked for 30 min in 3% (wt/vol) bovine serum albumin (BSA) and 5% (vol/vol) normal goat serum. Incubation with purified IgGs from ALS patients or control subjects at the appropriate dilutions (1 : 10 to 1 : 100) was performed for 16–20 h at 4°C in PBS containing 3% BSA, 0.1 M L-lysine and 0.075% (vol/vol) Triton X-100. Binding of the primary antibody was revealed by using a goat anti-human IgG coupled to fluorescein-isothiocyanate at a 1 : 2000 dilution. Co-staining with tetramethyl-rhodamine (TMR)-conjugated α-bungarotoxin (0.25 μg/mL) allowed us to identify NMJs through its high affinity for the post-synaptic nicotinic acetylcholine receptors. After extensive washing with PBS, sections were mounted in PBS-glycerol (1 : 1), covered with coverslips and sealed with nail polish. To check for non-specific binding and autofluorescence, controls were performed by omission of α-bungarotoxin, primary (isotype control) or secondary antibody.

Spinal cord, brain and cerebellum immunofluorescence

Tribromoethanol-anesthetized mice were transcardially perfused with PBS followed by 4% (wt/vol) paraformaldehyde-4% (wt/vol) sucrose after loss of both toe pitch and pupil-closing reflexes. After dissection of whole brain, cerebellum and spinal cord, tissue samples were additionally fixed in the same solution for 2–4 h at 4°C. Sections of 150 μm were obtained with an Integraslice 7550PSDS vibrating microslicer (Campden Instruments, Loughborough, UK) and subsequently permeabilized with 1% (vol/vol) Triton X-100 for 30 min. Incubation with purified IgGs from ALS patients or control subjects at a concentration of 0.2 mg/mL was performed for 16–20 h at 4°C in PBS containing 3% BSA (wt/vol), 0.1 M L-lysine and 0.075% (vol/vol) Triton X-100. Binding of primary antibody was detected using a goat anti-human IgG conjugated to fluorescein-isothiocyanate (1 : 2000 dilution). For spinal cord immunolabeling, thoracic and lumbar sections were analyzed because of the large size of cells in these regions. Lower motoneurons were detected by their morphology and localization at the ventral horn. The cortical primary motor area in slices was identified using a mouse brain atlas (Paxinos and Franklin 2001), while motoneurons were localized by size and shape. Purkinje neurons were recognized within cerebellar sections by means of their distinctive morphology. Subsequent distinction of molecular and granular cell layers was performed. In some cases, counter-staining with propidium iodide (3 μM, 60 min) was employed to distinguish different cellular populations by their morphology. In fixed tissues, propidium iodide stains citoplasm and nucleus due to its general affinity for nucleic acids.

Immunofluorescence analysis and image processing

Immunofluorescence staining was assessed using a FV300 confocal fluorescence microscope (Olympus Optical Co., Tokyo, Japan) equipped with an image acquisition system and Fluoview 3.3 software (Olympus Optical Co.). Sequential scanning of slices with Argon (λ: 488 nm) and Helium-Neon (λ: 543 nm) lasers was performed to reduce bleed-through of the fluorescence signal. Laser intensity as well as voltage, gain and offset configuration of each photomultiplier were kept constant for each experiment. An Olympus 60× oil-immersion PlanApo objective (numerical aperture: 1.4) was employed for analysis of coverslipped NMJ cryosections, whereas thick slices were kept in a Petri dish with PBS and photographed with an Olympus 60× water-immersion LUMplanFL objective (numerical aperture: 0.9), while immobilized with a slice hold-down device. Stacks of 10 confocal planes (1-μm interval) were acquired for each channel and subsequently analyzed with ImageJ 1.42 software (National Institutes of Health, Bethesda, MD, USA). Fluorescence intensity quantification was carried out by measuring mean grey values of at least 15 cells or NMJs from two to three different animals, after background subtraction. In the case of muscle preparations, the regions of interest were chosen based on the α-bungarotoxin signal. Mean gray values for each sample were normalized to the isotype control.

Cell culture and transfection/induction

Human embryonic kidney 293 (HEK293) cells [passage 18–26, American Type Culture Collection (ATCC) number CRL-1573] were maintained by serial passages in 75-cm^2 culture flasks. Cells were grown in Dulbecco's Modified Eagle's Medium containing 4 mM L-glutamine, 4.5 g/L glucose, 4 mg/L pyridoxine-HCl and 110 mL/L sodium pyruvate, supplemented with 10% heat-inactivated fetal bovine serum at 37°C in a humidified incubator with 5% CO_2 and 95% air. Sub-culturing of cells was performed with 0.25% trypsin-EDTA, followed by protease inactivation with Dulbecco's modified Eagle's medium containing fetal bovine serum and reseeding into 25-cm^2 culture flasks. Cultures at ~50% confluency were used for transfection experiments using Lipofectamine 2000 (Invitrogen, Carlsbad, CA, USA) following the manufacturer's instructions. Full-length human $Ca_V2.1$, and rat β_{2a} and $\alpha_2\delta_2$ cDNAs were contained in pcDNA3.1Zeo(+) (Invitrogen). Approximately 36 h post-transfection cells were processed for immunoprecipitation and/or western blot experiments.

Culturing of HEK293-derived T-rex 293 cells (passage 9–12) stably expressing the P/Q-type channel subunits was essentially the same as described above, except for the addition of 1% non-essential amino acids and, 24 h prior to induction, the addition of induction/selection agents Blasticidine (10 μg/mL), Zeocin (200 μg/mL) and Hygromycin B (150 μg/mL). In these cells, the pcDNA5/TO vector (Invitrogen) containing a tetracycline-responsive element was used to drive expression of the full-length $Ca_V2.1$ subunit, whereas the auxiliary subunits β_{2a} and $\alpha_2\delta_2$ were expressed in pBudCE4.1 (Invitrogen). Cells were lysed 48 h after induction with Tetracycline (1.5 μg/mL).

Crude membrane fraction preparation

Mouse cerebellum was disrupted with a glass-Teflon homogenizer in 4°C buffer containing 0.32 M sucrose in 50 mM Tris–HCl (pH 7.4). Homogenates were centrifuged at 1950 *g* for 10 min at 4°C and the resulting supernatant was spun down at 24 500 *g* for 20 min at 4°C. Pellets were resuspended in radio immunoprecipitation assay buffer (50 mM Tris–HCl buffer pH 8.0, 150 mM NaCl, 1% NP-40, 0.1% SDS and 0.5% sodium deoxycholate) with protease inhibitors (10 μM EDTA, 2 mM phenylmethylsulfonyl fluoride, 10 μg/mL aprotinin, 100 μM leupeptin, and 1 μg/mL pepstatin). Protein concentrations were determined by the Bradford (1976) assay.

Immunoprecipitation assay

Two-hundred micrograms of proteins were incubated overnight with ALS–IgGs (4 μg) and 60 μL of Protein G Plus-agarose beads (Santa

Cruz Biotechnology, Santa Cruz, California, USA), in a mixing rotor at 4°C. Beads were then washed with NP-40-containing lysis buffer (50 mM Tris-HCl buffer pH 7.4, 0.5% NP-40, 150 mM NaCl and 50 mM EDTA) and protein complexes interacting with the antibodies eluted with Laemmli buffer (62.5 mM Tris-HCl buffer pH 6.8, 2% SDS, 0.01% bromophenol blue, 2% β-mercaptoethanol and 10% glycerol) supplemented with protease inhibitors. Immunoprecipitates were analyzed by electrophoresis followed by western blot. An aliquot of the lysate originally used for each assay was run in parallel to check for the presence of the analyzed proteins (input), as well as a control by omission of antibodies (beads).

Gel electrophoresis and western blot

Western blots were performed according to standard procedures. In brief, cells were resuspended in Laemmli buffer containing protease inhibitors and mechanically disrupted using needles of decreasing internal diameter (26–29 G). Proteins were resolved by 4–12% Nu-polyacrylamide gradient gel electrophoresis (Nu-PAGE) and transferred onto nitrocellulose membranes (Amersham Hybond ECL; GE Healthcare, Piscataway, NJ, USA). Non-specific binding was blocked by 2% non-fat powdered milk in PBS containing 0.2% Tween-20 for 60 min at 20–23°C. Membranes were incubated overnight at 4°C with primary antibodies as described in Results, followed by addition of horseradish peroxidase-conjugated secondary antibodies. All antibodies were diluted in PBS containing 0.2% Tween-20 with 2% non-fat powdered milk. Immunoreactive bands were detected by chemiluminescence using horseradish peroxidase-conjugated secondary antibodies and a Supersignal Chemi-Luminescence detection kit (Pierce, Rockford, IL, USA) following the manufacturer's instructions.

Statistical analysis

Results are expressed and plotted as mean ± standard error of the mean (SEM) values. Experimental differences between groups were analyzed by the Mann–Whitney Rank Sum test or two-way analysis of variance (ANOVA) followed by Student–Newman–Keuls post-test where appropriate, with SigmaStat 3.5 software (Systat Software Inc.). A p-value of less than 0.05 was considered as statistically significant.

Materials

Tribromoethanol was purchased from Aldrich (Milwaukee, WI, USA). BSA, normal goat serum, TMR-tagged α-bungarotoxin and other chemicals were analytical grade and obtained from Sigma (St Louis, MO, USA). Goat anti-human secondary antibody (catalog number 1201-0081) was obtained from Cappel (Organon Teknika Corp., Arnhem, The Netherlands) whereas HiTrap ProteinG-Agarose columns were from GE Healthcare Bio-Sciences AB (Uppsala, Sweden).

Results

ALS–IgGs increased neuromuscular spontaneous synaptic activity and were able to bind to mouse neuromuscular junctions

To determine whether ALS–IgGs from our set of patients were able to modify MEPP frequency, we incubated diaphragm muscle preparations and analyzed spontaneous acetylcholine release using intracellular recordings. Figure 1 shows that 63% of the ALS patients tested (five of eight) possessed serum antibodies that significantly increased the frequency of MEPPs in mouse diaphragm from a resting state of ~30 MEPPs/min to a 2- to 5-fold increase (Rank Sum test, $p < 0.05$ comparing initial and final frequency). The enhanced effect on MEPPs was completely absent in experiments using any of RN, healthy or disease control IgGs (Rank Sum test, $p > 0.05$ comparing initial and final frequencies). This lack of effect was also observed in the three remaining ALS–IgGs, which were unable to raise spontaneous synaptic activity above basal levels (Rank Sum test, $p > 0.05$ comparing initial and final frequencies).

To gain a better understanding of the sites of action of the reactive antibodies, we performed indirect immunofluo-

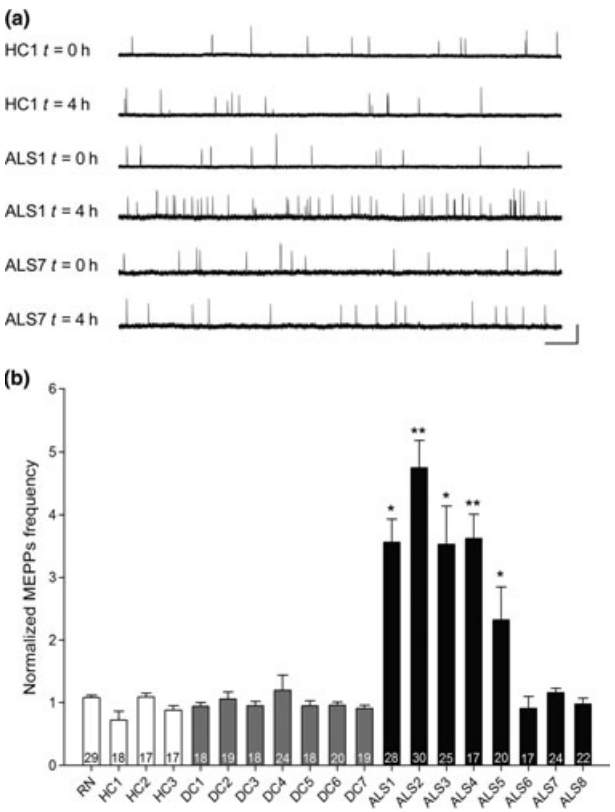

Fig. 1 MEPPs recordings of Swiss mice (P > 30) diaphragm preparations. Muscles were incubated with RN or with purified IgGs from ALS patients (ALS), healthy (HC) or disease controls (DC). (a) Representative intracellular recordings acquired before ($t = 0$ h) or after ($t = 4$ h) IgG incubation. Bar: 1 mV, 2 s. (b) MEPPs frequency quantification relative to the beginning of the experiment. Statistically significant differences after incubation time were detected by Rank Sum test. *$p < 0.05$ and **$p < 0.001$ compared with initial MEPP frequency. Numbers inside bars indicate the number of NMJs studied in each experimental condition.

rescence using IgGs from ALS or control individuals as primary antibodies, and α-bungarotoxin coupled to TMR as a post-synaptic marker of NMJs. Of note, Figs 2 and 3 show that the same set of five ALS–IgGs that produced synaptic potentiation also presented strong immunoreactivity against wild-type (WT) mouse diaphragm NMJs. Fluorescence intensities ranged from 3 to 22 times higher than those found for control subjects (Fig. 3, Rank Sum test, $p < 0.05$ comparing ALS and HCs). Conversely, NMJ reactivity for the remaining ALS–IgGs was not significantly different from healthy control samples (Rank Sum test, $p > 0.05$ comparing ALS and HCs). Although most of the control samples remained within non-specific binding levels, two of six disease controls also gave a positive result in this immunolabeling assay (Rank Sum test, $p < 0.01$ comparing disease samples and HCs). These sera belonged to patients with known autoimmune diseases directed against NMJ components, such as Lambert-Eaton myasthenic syndrome (DC1) and myasthenia gravis (DC2). A further aspect worth noting is the lack of electrophysiological effect and NMJ binding in all of the fALS samples tested (DC4-6; Figs 1b and 3).

ALS–IgGs reactivity towards $Ca_V2.1^{-/-}$ and $Ca_V2.2^{-/-}$ mouse neuromuscular junctions

We started evaluating whether the presence or absence of P/Q-type and N-type α_1 subunits affected ALS–IgGs reactivity. As shown in Fig. 4a, ALS–IgGs reactivity was almost completely absent when diaphragm muscles from animals null for the P/Q-type $Ca_V2.1$ subunit were examined (two-way ANOVA followed by Student–Newman-Keuls post-test, $p < 0.001$ comparing WT and null animals). In the $Ca_V2.1^{-/-}$ animals, fluorescence intensity values were not statistically different from those obtained using control IgGs (Fig. 4b, two-way ANOVA followed by Student–Newman–Keuls post-test, $p > 0.05$ comparing ALS–IgGs and healthy control IgGs). In contrast, antibodies from the disease controls which showed affinity for WT NMJs (DC1 and DC2, Fig. 3) exhibited strong affinity to sections from both WT and $Ca_V2.1$-null animals (Fig. 4b, two-way ANOVA followed by Student–Newman–Keuls post-test, $p > 0.05$ comparing WT and $Ca_V2.1^{-/-}$ animals).

In contrast to that for the P/Q-type channel, there was no difference in ALS–IgGs immunoreactivity in mice either WT or null for the N-type $Ca_V2.2$ Ca^{2+} channel subunit. Figure 5 shows that interaction of most ALS antibodies with NMJs was present at similar levels for both genotypes (two-way ANOVA followed by Student–Newman–Keuls post-test, $p > 0.05$ comparing WT and null muscles), except for ALS2 and ALS7 which displayed a small but significant decrease and increase in NMJ immunolabeling, respectively (two-way ANOVA followed by Student–Newman–Keuls post-

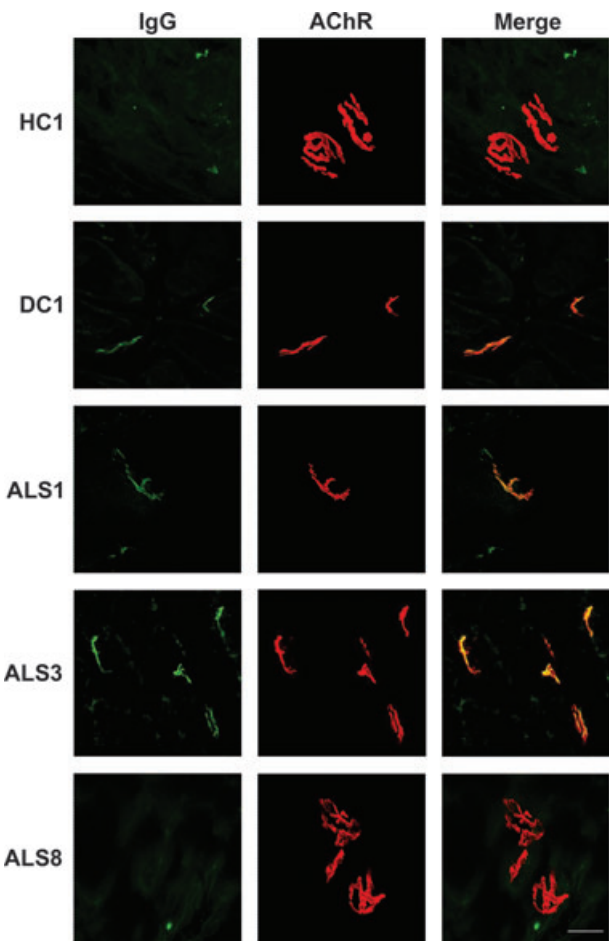

Fig. 2 Immunofluorescence of Swiss mice (P > 30) diaphragm sections (40 μm) incubated with purified IgGs from HC, DC or ALS. Visualization of the primary antibody was performed by anti-human IgG coupled to FITC. Alpha-bungarotoxin tagged with TMR was used as a post-synaptic marker of NMJs (AChR, acetylcholine receptor). Pictures in the last column show superimposed images. Bar: 25 μm.

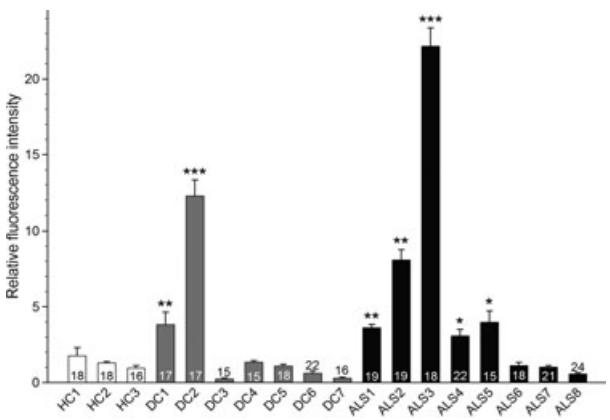

Fig. 3 Fluorescence intensity quantification of Swiss mice (P > 30) diaphragm sections incubated with purified IgGs from HC, DC or ALS. Data are normalized to isotype control. Statistical analysis was performed by Rank Sum test. *$p < 0.05$, **$p < 0.01$ and ***$p < 0.001$ compared with HCs. Figures inside bars indicate the number of NMJs studied in each experimental condition ($N = 7$ animals).

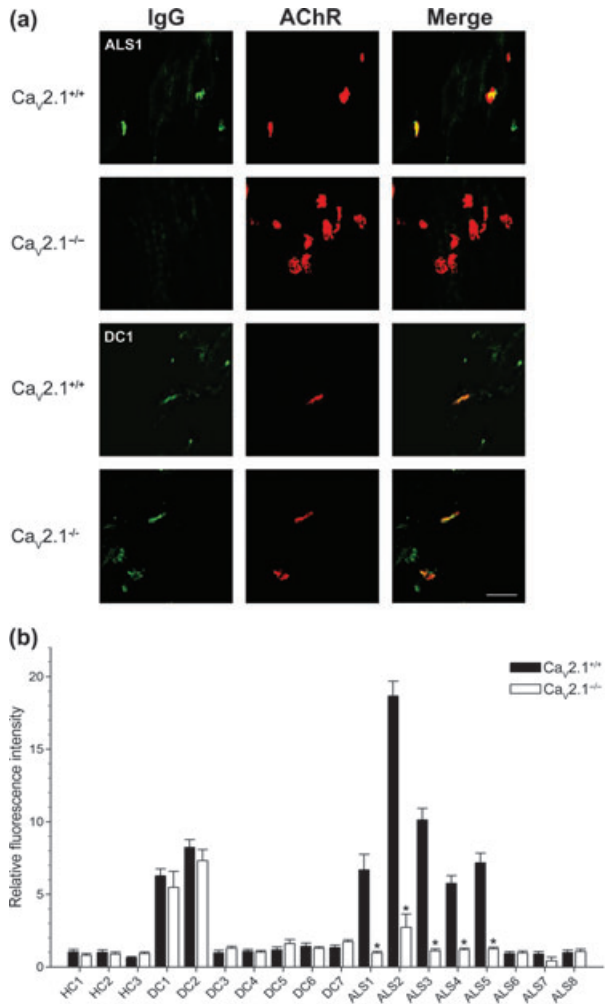

Fig. 4 Diaphragm sections (40 μm) from WT or $Ca_V2.1^{-/-}$ mice (P16-23), incubated with purified IgGs from HC, DC or ALS. Presence of primary antibody was determined as previously described. (a) Representative confocal micrographs of NMJ. The smaller size of end-plates compared with Fig. 2 is due to the younger age of animals. Bar: 25 μm. (b) Fluorescence intensity determinations normalized to isotype control. Statistical analysis between WT and $Ca_V2.1$-null muscles was performed by two-way ANOVA. $^*p < 0.001$ compared with WT. The number of NMJs studied in each experimental condition varied between 16 and 30 ($N = 5$ animals).

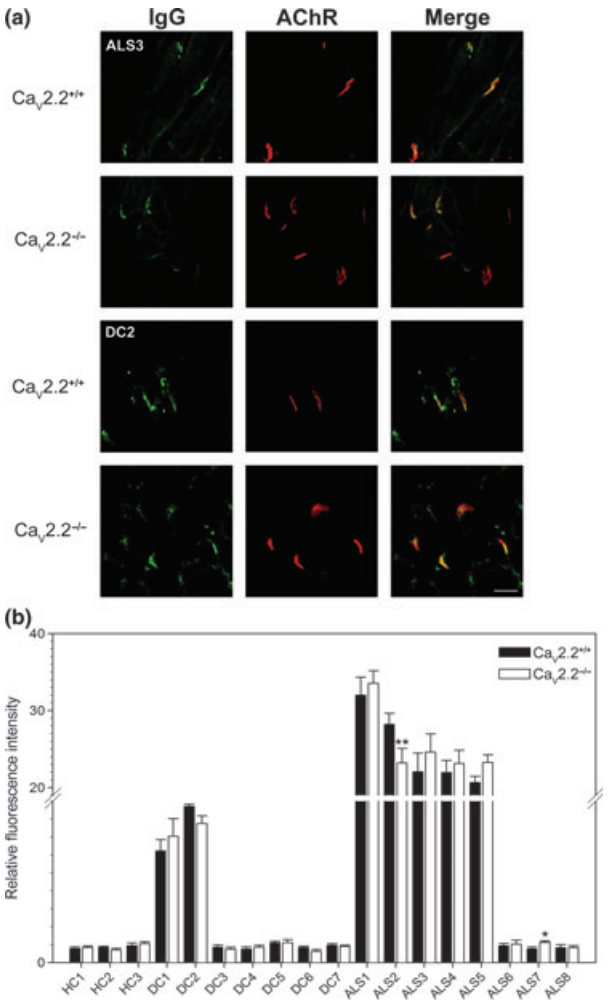

Fig. 5 Immunofluorescence of diaphragm sections (40 μm) from WT or $Ca_V2.2^{-/-}$ mice (P18), incubated with purified IgGs from HC, DC or ALS. Visualization of primary antibody was performed as previously described. (a) Representative NMJ pictures. The smaller size of end-plates compared with Fig. 2 is due to the younger age of animals. Bar: 25 μm. (b) Fluorescence intensity quantification normalized to isotype control. Statistical analysis between WT and $Ca_V2.2$-null muscles was performed by two-way ANOVA. $^*p < 0.05$ and $^{**}p < 0.01$ compared with WT. The number of NMJs studied in each experimental condition varied between 15 and 25 ($N = 4$ animals).

test, $p < 0.01$ for ALS2 and $p < 0.05$ for ALS7, comparing WT and null muscles). Additionally, neither of the disease controls that reacted against WT end-plates (DC1 and DC2) exhibited any difference in immunoreactivity in N-type $Ca_V2.2$-null samples (Fig. 5b, two-way ANOVA followed by Student–Newman–Keuls post-test, $p > 0.05$ comparing WT and null animals).

ALS–IgGs functionality on $Ca_V2.1$-null mice spontaneous neuromuscular activity

To evaluate the functional relevance of the diminished ALS–IgG interaction found for $Ca_V2.1$-null NMJs, we next tested for effects on spontaneous synaptic activity. Because of sample shortage, we could not include in this study all of the ALS–IgGs previously assessed. After a 4-h incubation period, two of four ALS samples (ALS2 and ALS5) were found to significantly increase acetylcholine release in WT diaphragm to frequencies 40–60 times higher than initial values (Fig. 6a and b, two-way ANOVA followed by Student–Newman–Keuls post-test, $p < 0.001$ comparing WT and null mice). Although sv129 mice muscles resulted more sensitive to ALS–IgGs modulatory effects than Swiss mice diaphragms (Fig. 1), it is important to emphasize that both results are essentially in accordance.

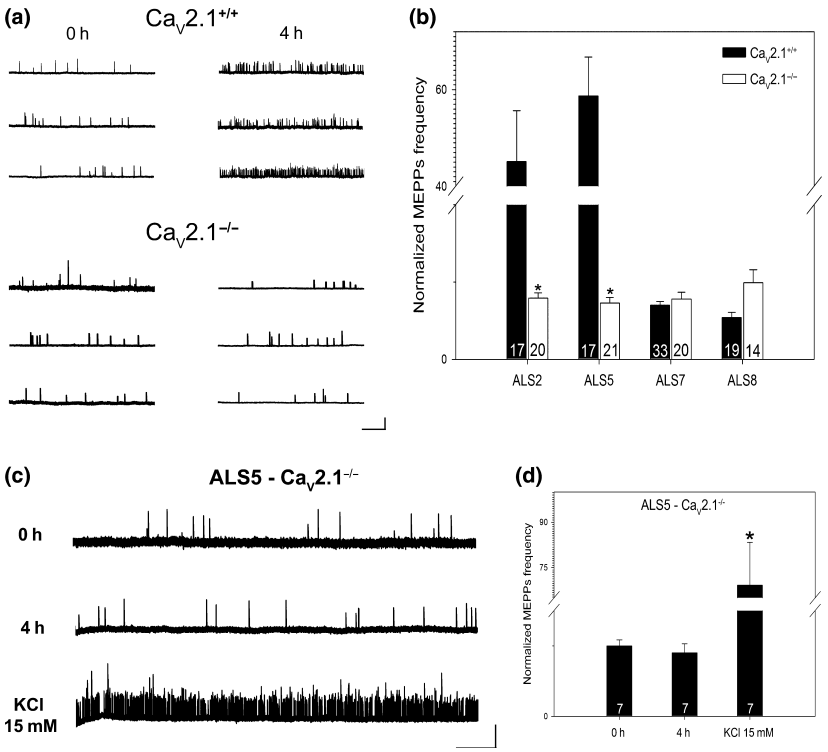

Fig. 6 MEPPs recordings of mouse diaphragm preparations from WT or $Ca_V2.1$-null animals (P16-22). Muscles were incubated with purified IgGs from ALS patients (ALS). (a) Representative intracellular recordings acquired before ($t = 0$ h) or after ($t = 4$ h) IgG incubation (ALS2). Bar: 2 mV, 5 s. (b) MEPPs frequency quantification relative to the beginning of the experiment. Statistically significant differences after incubation time between genotypes were detected by two-way ANOVA. *$p < 0.001$ compared with WT frequency. Figures inside bars indicate the number of NMJs studied in each experimental condition. (c) Representative intracellular recordings of $Ca_V2.1$-null muscles. Tissue was subsequently incubated with ALS5-IgGs for 4 h and a 15 mM-KCl solution for 10 min. Bar: 2 mV, 5 s. (d) MEPPs frequency quantification relative to the beginning of the experiment. Statistically significant differences after treatments were detected by Rank Sum test. *$p < 0.001$ compared with initial and 4-h frequency. Figures inside bars indicate the number of NMJs studied in each experimental condition.

Those antibodies that promoted an increase in NMJ neurotransmitter release were unable to increase MEPPs frequency above initial values in muscles from $Ca_V2.1^{-/-}$ animals (Fig. 6a and b, two-way ANOVA followed by Student–Newman–Keuls post-test, $p > 0.05$ comparing WT and $Ca_V2.1^{-/-}$ mice). However, all the $Ca_V2.1$-null diaphragm preparations retained their ability to respond to a depolarizing stimulus (15 mM KCl) by significantly increasing spontaneous acetylcholine release after a 10-min incubation period (Fig. 6c and d, Rank Sum test, $p < 0.001$ comparing initial, 4-h and KCl frequencies).

CNS: cerebellar, cortical and spinal cord immunolabeling

Immunofluorescence experiments performed on mouse spinal and brain cortical slices showed that the majority of ALS–IgGs (six of eight) had affinity for antigens present in the soma of Purkinje neurons (Figure S1a and b, Rank Sum test, $p < 0.05$ comparing ALS and HCs), as well as for motoneurons located at the spinal ventral horn (Figure S1c and d, Rank Sum test, $p < 0.01$ comparing ALS and HCs). In contrast, no reactivity was observed when healthy control IgGs were examined (Figure S1). Furthermore, when the presence of immunoreactivity was evaluated in slices of primary motor cortex, neither samples from ALS patients nor control subjects exhibited differences compared to non-specific control binding (data not shown).

We next assessed whether antibody interactions with neuronal structures was altered in $Ca_V2.1^{-/-}$ animals. Unlike that for NMJs, the absence of the P/Q-type channel $Ca_V2.1$ subunit did not decrease either cerebellar or spinal cord immunolabeling when compared to WT mice slices (Figure S2; two-way ANOVA followed by Student–Newman–Keuls post-test, $p > 0.05$ comparing WT and null animals). This unexpected result suggests the existence of antigens reactive to ALS–IgGs at peripheral and central synaptic locations that are differentially affected by the expression of intact P/Q-type channels.

Analysis of ALS–IgGs interaction with the P/Q-type Ca^{2+} channel α_1 subunit and other pre-synaptic proteins

Our results indicating that IgGs from a subset of sALS patients strongly react with wild-type mouse NMJs (both by

immunofluorescence signal and functional effects on MEPP frequency) but not with end-plates from P/Q-type channel-null animals, together with a lack of immunostaining difference across CNS targets in $Ca_V2.1^{-/-}$ versus $Ca_V2.1^{+/+}$ animals, prompted us to more directly evaluate the interactions between ALS–IgGs and P/Q-type Ca^{2+} channels. To this aim we transfected HEK cells with full-length $Ca_V2.1$, β_{2a} and $\alpha_2\delta_2$ cDNAs and analyzed cell lysates by western blot. None of the evaluated ALS–IgG samples exhibited affinity towards the human $Ca_V2.1$ pore-forming or ancillary subunits exogenously expressed in HEK cells (Figure S3a). There was some reactivity towards an unknown protein of molecular weight ~130 kDa (similar to the molecular weight of the $\alpha_2\delta_2$ subunit), although this antigen was also present in non-transfected cells (Figure S3b).

We next attempted to immunoprecipitate exogenously expressed P/Q-type channel subunits with ALS–IgGs. Although the human $Ca_V2.1$ subunit was easily detectable in the original lysate, the ALS–IgGs tested did not exhibit noticeable interaction with the channel (Figure S3c). Similarly negative results were found when performing immunoprecipitation experiments with a HEK293-derived cell line stably expressing the P/Q-type channel subunit complex (Figure S3d and e).

We also evaluated several ALS–IgG samples for reactivity against other pre-synaptic proteins, including synaptotagmin I, syntaxin 1A, synaptophysin and synaptobrevin II, using cerebellar synaptosomal extracts as a protein source for the immunoprecipitation assay. In none of the tested cases we were able to detect an interaction between the analyzed ALS–IgGs and the synaptic components (Figure S3f), although they were all easily detectable either in the input fraction or in the positive controls (PRE).

Discussion

In the present study, we demonstrated the existence of a subpopulation of sALS patients (63% in our sample), whose IgG fractions induced a significant enhancement of spontaneous acetylcholine release (Fig. 1). A similar effect has been postulated to be the consequence of increased intracellular Ca^{2+} at nerve terminals caused by ALS–IgG binding to targets in presynaptic membranes (Uchitel *et al.* 1988, 1992b; Pagani *et al.* 2006). IgGs from the same set of sALS patients also exhibited strong immunolabeling in wild-type mouse NMJs (Figs 2 and 3). Together, our results reinforce those of Pagani *et al.* (2006) who found an association between ALS–IgG binding and electrophysiological effects. From our data, it is also apparent that it is possible to separate sALS patients into two groups; one of which appears to have a strong autoimmune, neuromuscular-related component and that might contribute towards disease neuropathology.

There is a growing body of evidence supporting a role for Ca^{2+}-dependent signaling as an important regulator of cellular dysfunction and death (Appel *et al.* 2001; Orrenius *et al.* 2003). Furthermore, spinal motoneurons are known to be particularly vulnerable to Ca^{2+} imbalance caused by their diminished expression of Ca^{2+}-buffering proteins (Alexianu *et al.* 1994). An increase in intracellular Ca^{2+} levels above a certain threshold is predicted to trigger processes such as calpain activation, protein misfolding-endoplasmic reticulum stress, reactive oxygen species production and glutamate release (Orrenius *et al.* 2003; Smaili *et al.* 2009). The stimulation of any of these pathways via an aberrant rise in intracellular Ca^{2+} concentration could lead to the induction of apoptosis and provide a key link underlying ALS pathology. Additionally, reports documenting an enhancement in Ca^{2+} content of motoneurons and synaptic terminals in mice injected with ALS–IgGs have provided a key connection between Ca^{2+} overload and ALS (Engelhardt *et al.* 1995; Pullen and Humphreys 2000).

The comparison of ALS–IgG reactivity levels against NMJ (Fig. 3) and their potentiator effect on end-plate basal discharge activity (Fig. 1) indicates that both characteristics show a basically similar behavior, even though their sensitivities seem to be moderately different. Apart from differences in the intrinsic sensitivity of each technique employed, the discrepancy might also arrive as a consequence of the presence in some samples of several antibodies capable of interacting with the motor terminals.

The presence of significant levels of immunoreactivity in some disease controls was not unexpected (Figs 2–5 and Figures S1 and S2), as these individuals might have antibodies against proteins involved in synaptic transmission (i.e. voltage-dependent Ca^{2+} channels in DC1 and acetylcholine receptors in DC2). In this way, these samples serve as useful positive controls for the immunohistochemical techniques used to detect autoantibodies in sALS samples. Another important aspect to consider is the complete lack of reactivity in all the fALS samples analyzed (Fig. 3), as well as their inability to affect end-plate spontaneous synaptic activity (Fig. 1b). These results emphasize the specificity of our findings concerning sALS immunoglobulins since it is known that the hereditary form of the disease is clinically indistinguishable from the sporadic variant.

The finding that the IgG sample from DC1 (a Lambert-Eaton myasthenic syndrome patient) exhibited a similar level of interaction with $Ca_V2.1^{+/+}$ and $Ca_V2.1^{-/-}$ end-plates might seem contradictory at first sight, because of the proposed etiology for this disease. However, it should be stressed that this sample might contain antibodies against not only $Ca_V2.1$ Ca^{2+} channels but also $Ca_V2.2$ (Takamori *et al.* 1995; Motomura *et al.* 1997). This latter channel is known to compensate for the lack of P/Q-type channels, both at the functional (Urbano *et al.* 2003) and proteic level (Pagani *et al.* 2004), and therefore could explain the invariability observed in immunostaining.

To further characterize ALS antibody reactivity against other neuronal substrates possibly relevant to disease pathophysiology, we performed immunofluorescence assays on mouse spinal and brain cortical slices. These neural structures are the site of residence for lower and upper motoneurons, respectively, both of which are important movement effectors. Cerebellar structures were also analyzed since they comprise cells involved in movement coordination and it has been shown that ALS antibodies are capable of modulating P/Q-type Ca^{2+} currents (Llinas *et al.* 1993). We found a broad reactivity pattern for ALS–IgGs in neuronal tissues such as the cerebellum and spinal cord (Figure S1), in which the vast majority of samples analyzed resulted in positive staining. Of note, we could not detect any difference in the reactivity of ALS–IgGs when comparing WT to $Ca_V2.1$-null animals in these regions (Figure S2). These data are in striking contrast to the clear differences detected in immunofluorescence experiments performed on NMJs (Fig. 4), and thus highlight the specificity of the findings for end-plate preparations. Along these lines, we speculate that the antigen(s) responsible for ALS–IgG labeling motor terminals is(are) predominantly expressed in these more peripheral synaptic sites than others such as the cerebellum or spinal ventral horn. However, we cannot exclude the possibility that the presence of the ALS–IgG reactive antigen(s) could be masked by other antigens expressed in the cerebellar or spinal cord neurons and which are more abundant or reactive towards ALS–IgGs. Additionally, the presence in ALS sera of such CNS-reactive antibodies is more likely the consequence of intracellular content exposure caused by neuronal injury, owing to their broad distribution amongst several ALS samples and the lack of correlation with NMJ binding.

As P/Q-type channels are the principal mediators of synaptic transmission in mammalian NMJs (Uchitel *et al.* 1992a; Katz *et al.* 1997) and there is evidence supporting an interaction between ALS–IgGs and Ca^{2+} channels (Llinas *et al.* 1993; Smith *et al.* 1994; Carter and Mynlieff 2003), we analyzed the effects of ALS–IgGs on deleting the $Ca_V2.1$ subunit. Our results showed that the absence of the P/Q-type channel $Ca_V2.1$ subunit produced a significant decrease in ALS–IgG binding to mouse NMJs (Fig. 4), as well as the complete suppression of ALS–IgG-mediated effects on enhancing spontaneous acetylcholine release (Fig. 6). Taken together, these data suggested that a subset of ALS–IgGs interact with either the $Ca_V2.1$ subunit or other protein(s) whose expression in NMJs is dramatically diminished as a consequence of $Ca_V2.1$ subunit deletion. In support of the latter, it is known that $Ca_V2.1$ subunit-null mice exhibit alterations in the expression of other genes besides the $Ca_V2.1$ subunit (Piedras-Renteria *et al.* 2004). Furthermore, other reports suggest that Ca^{2+} influx through P/Q-type channels – and hence, their presence and functionality – might be an important factor relevant to the transcription of synapse-related genes such as the soluble *N*-ethylmaleimide sensitive factor attachment protein receptor (SNARE) protein syntaxin 1A (Sutton *et al.* 1999; Barbado *et al.* 2009).

A microarray analysis of the $Ca_V2.1$ gene (*CACNA1A*) expression profile revealed a seven-fold decrease in $Ca_V2.1$ messenger ribonucleic acid levels in rat extraocular muscle compared with a typical skeletal muscle such as *tibialis anterior* (Fischer *et al.* 2002). The extraocular muscle is well-known for being relatively spared during ALS progression (Leveille *et al.* 1982) and has been reported to be resistant to ALS–IgG NMJ effects in passive transfer experiments (Mosier *et al.* 2000). These studies provide a further important link between P/Q-type channel expression and ALS susceptibility.

Distinct from the above arguments in favor of a direct role of functional P/Q-type channels, our immunoprecipitation and western blot experiments using HEK293 cells expressing cloned P/Q-type channel subunits do not support a direct interaction of ALS–IgGs with the channel complex itself (Figure S3), at least under the conditions analyzed for this study. In support, ALS–IgGs have been shown not to interact with ^{125}I-ω-conotoxin MVIIC-labeled channels (Drachman *et al.* 1995) and also that P/Q-type channel inhibition by ω-agatoxin IVA did not prevent immunoglobulin-induced synaptic potentiation (Pagani *et al.* 2006). Taken together, our results suggest that the protein(s) interacting with ALS–IgGs requires $Ca_V2.1$ expression/activity at the NMJ although it is $Ca_V2.1$-expression independent in other neuronal structures such as the cerebellum and spinal cord.

Another aspect worth noting is the lack of change in antibody binding to $Ca_V2.1^{-/-}$ NMJ for disease control sera compared to WT conditions (Fig. 4b). This invariability in immunostaining adds relevance to ALS–IgG findings by highlighting their specificity towards a selected subset of patients.

N-type Ca^{2+} channel activation has been found to be relevant for the induction of spontaneous synaptic activity by ALS–IgGs (Pagani *et al.* 2006). However, this effect is unlikely the consequence of a direct interaction between antibodies and the $Ca_V2.2$ N-type subunit as the loss of $Ca_V2.2$ did not significantly alter IgG binding of most of the ALS samples at mouse NMJs (Fig. 5). Moreover, it has been shown that in $Ca_V2.1$-null mutant animals, there is a functional compensation in neuromuscular transmission by N-type Ca^{2+} channels (Urbano *et al.* 2003), as well as an increment in channel protein levels (Pagani *et al.* 2004). Therefore, this could explain the significant changes in ALS–IgG immunoreactivity noted here (Fig. 4). Together, these results do not support a direct binding of ALS antibodies to the N-type channel but rather an indirect effect of IgGs on channel activity, for example through a second messenger signaling pathway, as it has been extensively reported for this channel (Lipscombe *et al.* 1989; Werz *et al.* 1993; Martin *et al.* 2006). In fact, Pagani *et al.* (2006) did detect a requirement of phospholipase C, ryanodine receptor and

inositol triphosphate receptor activation for the ALS–IgG-induced synaptic potentiation to occur.

Several reports have documented the presence of human antibodies at the motoneuronal soma and nerve terminals of mice injected with ALS–IgGs (Fratantoni *et al.* 1996; Engelhardt *et al.* 2005), we speculated it might be the consequence of an interaction between disease antibodies and pre-synaptic components. In order to test this possibility, we assessed by immunoprecipitation experiments ALS–IgGs binding to several pre-synaptic proteins purified from synaptosomal extracts. We found that none of the evaluated ALS samples showed affinity towards proteins present at synaptic terminals, such as synaptotagmin I, syntaxin 1A, synaptophysin and synaptobrevin II, all of which were readily detectable in the original lysates (Figure S3f). Other candidates to test in the future include extracellular matrix molecules, neurotrophins receptors and proteins involved in synaptogenesis and axon guidance, due to their proposed role during neurodegeneration (Dawbarn and Allen 2003; Glas *et al.* 2007; Schmidt *et al.* 2009).

The results in the current work add relevant evidence in favor of autoimmunity as one of the possible mechanisms contributing to ALS pathology. They also suggest for the first time that, as opposed to generally interacting with all central and peripheral P/Q-type Ca^{2+} channels, autoantibodies in the serum of a subset of patients selectively interact with antigens at NMJs. The results also contribute towards further studies aimed at defining the IgGs as biological markers for sALS and in disease pathophysiology.

Acknowledgements

The authors are very grateful to Drs Joaquín Piriz, Francisco Urbano and Carina Weissmann for helpful comments on the manuscript and to María Eugenia Martín for technical assistance. We would also like to thank Drs John Tyson and Esperanza García for assistance with the transfection and immunoprecipitation experiments. We acknowledge the contribution of Dr Shin Hee-Sup for kindly providing the $Ca_V2.1^{-/-}$ and $Ca_V2.2^{-/-}$ mice. This work was supported by the National Agency for Scientific and Technological Promotion (Grant 32113, Argentina). Work in the laboratory of T.P. Snutch was supported by an operating grant from the Canadian Institutes of Health Research and a Tier 1 Canada Research Chair in Biotechnology and Genomics-Neurobiology. The authors declare no conflict of interests.

Supporting information

Additional supporting information may be found in the online version of this article:

Figure S1. Immunofluorescence of Swiss mice (P > 30) cerebellum and spinal cord slides (150 μm) incubated with purified IgGs from HC, DC or ALS.

Figure S2. Immunofluorescence of mouse cerebellum and spinal cord slides (150 μm) from WT or $Ca_V2.1^{-/-}$ mice (P16-23), incubated with purified IgGs from HC, DC or ALS.

Figure S3. Interaction of ALS antibodies with proteins from P/Q-type channel-expressing cells.

As a service to our authors and readers, this journal provides supporting information supplied by the authors. Such materials are peer-reviewed and may be re-organized for online delivery, but are not copy-edited or typeset. Technical support issues arising from supporting information (other than missing files) should be addressed to the authors.

References

Alexianu M. E., Ho B. K., Mohamed A. H., La Bella V., Smith R. G. and Appel S. H. (1994) The role of calcium-binding proteins in selective motoneuron vulnerability in amyotrophic lateral sclerosis. *Ann. Neurol.* **36**, 846–858.

Appel S. H., Stockton-Appel V., Stewart S. S. and Kerman R. H. (1986) Amyotrophic lateral sclerosis: associated clinical disorders and immunological evaluation. *Arch. Neurol.* **43**, 234–238.

Appel S. H., Engelhardt J. I., Garcia J. and Stefani E. (1991) Immunoglobulins from animal model of motor neurons disease and from human amyotrophic lateral sclerosis patients passively transfer physiological abnormalities to the neuromuscular junction. *Proc. Natl Acad. Sci. USA* **88**, 647–651.

Appel S. H., Smith R. G., Englehardt J. I. and Stefani E. (1993) Evidence for autoimmunity in amyotrophic lateral sclerosis. *J. Neurol. Sci.* **118**, 169–174.

Appel S. H., Beers D., Siklos L., Engelhardt J. I. and Mosier D. R. (2001) Calcium: the Darth Vader of ALS. *Amyotroph. Lateral Scler. Other Motor Neuron Disord.* **2**, S47–S54.

Arsac C., Raymond C., Martin-Moutot N., Dargent B., Couraud F., Pouget J. and Seagar M. (1996) Immunoassays fail to detect antibodies against neuronal calcium channels in amyotrophic lateral sclerosis serum. *Ann. Neurol.* **40**, 695–700.

Barbado M., Fablet K., Ronjat M. and De Waard M. (2009) Gene regulation by voltage-dependent calcium channels. *Biochim. Biophys. Acta* **1793**, 1096–1104.

Bourinet E., Soong T. W., Sutton K., Slaymaker S., Mathews E., Monteil A., Zamponi G. W., Nargeot J. and Snutch T. P. (1999) Phenotypic variants of P- and Q-type calcium channels are generated by alternative splicing of the α1A subunit gene. *Nat. Neurosci.* **2**, 407–415.

Bowling A. C., Schulz J. B., Brown R. H. and Beal M. F. (1993) Superoxide dismutase activity, oxidative damage and mitochondrial energy metabolism in familial and sporadic amyotrophic lateral sclerosis. *J. Neurochem.* **61**, 2322–2325.

Bradford M. M. (1976) A rapid and sensitive method for the quantification of microgram of protein utilizing the principle of protein-dye binding. *Anal. Biochem.* **72**, 248–254.

Brooks B. (1994) El Escorial World Federation of Neurology criteria for the diagnosis of amyotrophic lateral sclerosis. Subcommittee on Motor Neuron Diseases/Amyotrophic Lateral Sclerosis of the World Federation of Neurology Research Group on Neuromuscular Diseases and the El Escorial 'Clinical limits of amyotrophic lateral sclerosis' workshop contributors. *J. Neurol. Sci.* **142**, 96–107.

Carter J. R. and Mynlieff M. (2003) Amyotrophic lateral sclerosis patient IgG alters voltage dependence of Ca^{2+} channels in dissociated rat motoneurons. *Neurosci. Lett.* **353**, 221–225.

Couratier P., Yi F. H., Preud'homme J. L., Clavelou P., White A., Sindou P., Vallat J. M. and Jauberteau M. O. (1998) Serum autoantibodies to neurofilament proteins in sporadic amyotrophic lateral sclerosis. *J. Neurol. Sci.* **154**, 137–145.

Dawbarn D. and Allen S. J. (2003) Neurotrophins and neurodegeneration. *Neuropathol. Appl. Neurobiol.* **29**, 211–230.

Demestre M., Pullen A., Orrell R. W. and Orth M. (2005) ALS-IgG-induced selective motor neurone apoptosis in rat mixed primary spinal cord cultures. *J. Neurochem.* **94**, 268–275.

Drachman D. B. and Kuncl R. W. (1989) Amyotrophic lateral sclerosis: an unconventional autoimmune disease? *Ann. Neurol.* **26**, 269–274.

Drachman D. B., Fishman P. S., Rothstein J. D., Motomura M., Lang B., Vincent A. and Mellits E. D. (1995) Amyotrophic lateral sclerosis: an autoimmune disease? *Adv. Neurol.* **68**, 59–65.

Dubel S. J., Starr T. V. B., Hell J., Ahlijanian M. K., Enjeart J. J., Catterall W. A. and Snutch T. P. (1992) Molecular cloning of the alpha-1 subunit of an omega-conotoxin-sensitive calcium channel. *Proc. Natl Acad. Sci. USA* **89**, 5058–5062.

Engelhardt J. I. and Appel S. H. (1990) IgG reactivity in the spinal cord and motor cortex in amyotrophic lateral sclerosis. *Arch. Neurol.* **47**, 1210–1216.

Engelhardt J. I., Appel S. H. and Killian J. M. (1990) Motor neuron destruction in guinea pigs immunized with bovine spinal cord ventral horn homogenate: experimental autoimmune gray matter disease. *J. Neuroimmunol.* **27**, 21–31.

Engelhardt J. I., Siklós L., Kömüves L., Smith R. G. and Appel S. H. (1995) Antibodies to calcium channels from ALS patients passively transferred to mice selectively increase intracellular calcium and induce ultrastructural changes in motoneurons. *Synapse* **20**(3), 185–99.

Engelhardt J. I., Soos J., Obal I., Vigh L. and Siklos L. (2005) Subcellular localization of IgG from the sera of ALS patients in the nervous system. *Acta Neurol. Scand.* **112**, 126–133.

Fischer M. D., Gorospe J. R., Felder E., Bogdanovich S., Pedrosa F., Ahima R. S., Rubinstein N. A., Hoffman E. P. and Khurana T. S. (2002) Expression profiling reveals metabolic and structural components of extraocular muscles. *Physiol. Genomics* **9**, 71–84.

Fratantoni S. A., Dubrovsky A. L. and Uchitel O. D. (1996) Uptake of immunoglobulin G from amyotrophic lateral sclerosis patients by motor nerve terminals in mice. *J. Neurol. Sci.* **137**, 97–102.

Glas M., Popp B., Angele B., Koedel U., Chahli C., Schmalix W. A., Anneser J. M., Pfisterand H. W. and Lorenzl S. (2007) A role for the urokinase-type plasminogen activator system in amyotrophic lateral sclerosis. *Exp. Neurol.* **207**(2), 350–356.

Katz E., Protti D. A., Ferro P. A., Rosato Siri M. D. and Uchitel O. D. (1997) Effects of Ca^{2+} channel blocker neurotoxins on transmitter release and presynaptic currents at the neuromuscular junction. *Br. J. Pharmacol.* **121**, 1531–1540.

Leveille A. J., Ciernan A. J., Goodwin J. A. and Antel J. (1982) Eye movements in amyotrophic lateral sclerosis. *Arch. Neurol.* **39**, 684–686.

Lipscombe D., Kongsamut S. and Tsien R. W. (1989) Alpha-adrenergic inhibition of sympathetic neurotransmitter release mediated by modulation of N-type calcium-channel gating. *Nature* **340**(6235), 639–642.

Llinas R., Sugimori M., Cherksey B. D., Smith R. G., Delbono O., Stefani E. and Appel S. (1993) IgG from amyotrophic lateral sclerosis patients increases current through P-type calcium channels in mammalian cerebellar Purkinje cells and in isolated channels protein in lipid bilayer. *Proc. Natl Acad. Sci. USA* **90**, 11743–11747.

Martin S. W., Butcher A. J., Berrow N. S., Richards M. W., Paddon R. E., Turner D. J., Dolphin A. C., Sihra T. S. and Fitzgerald E. M. (2006) Phosphorylation sites on calcium channel alpha 1 and beta subunits regulate ERK-dependent modulation of neuronal N-type calcium channels. *Cell Calcium* **39**(3), 275–292.

Mendonca D. M. F., Chimelli L. and Martinez A. M. B. (2005) Quantitative evidence for neurofilament heavy subunit aggregation in motor neurons of spinal cords of patients with Amyotrophic Lateral Sclerosis. *Braz. J. Med. Biol. Res.* **38**, 925–935.

Mosier D. R., Bardelli P. and Delbono O. (1995) Amyotrophic lateral sclerosis immunoglobulins increase Ca^{2+} current in a motor neuron cell line. *Ann. Neurol.* **37**, 102–109.

Mosier D. R., Siklos L. and Appel S. H. (2000) Resistance of extraocular motoneuron terminals to effects of amyotrophic lateral sclerosis sera. *Neurology* **54**, 252–255.

Motomura M., Lang B., Johnston I., Palace J., Vincent A. and Newsom-Davis J. (1997) Incidence of serum anti-P/O-type and anti-N-type calcium channel autoantibodies in the Lambert-Eaton myasthenic syndrome. *J. Neurol. Sci.* **147**(1), 35–42.

Mulder D. W. (1982) Clinical limits of amyotrophic lateral sclerosis. *Adv. Neurol.* **36**, 15–22.

Niebroj-Dobosz I., Dziewulska D. and Kwiecinski H. (2004) Oxidative damage to proteins in the spinal cord in amyotrophic lateral sclerosis. *Folia Neuropathol.* **42**, 151–156.

Orrenius S., Zhivotovsky B. and Nicotera P. (2003) Regulation of cell death: the calcium-apoptosis link. *Nature Rev.* **4**, 552–565.

Pagani M. R., Song M., McEnery M., Qin N., Tsien R. W., Toro L., Stefani E. and Uchitel O. D. (2004) Differential expression of α_1 and β subunits of voltage-dependent Ca^{2+} channel at the neuromuscular junction of normal and P/Q Ca^{2+} channel knockout mouse. *Neuroscience* **123**, 75–85.

Pagani M. R., Reisin R. C. and Uchitel O. D. (2006) Calcium signaling pathways mediating synaptic potentiation triggered by amyotrophic lateral sclerosis IgG in motor nerve terminals. *J. Neurosci.* **26**, 2661–2672.

Paxinos G. and Franklin K. B. J. (2001) *The Mouse Brain in Stereotaxic Coordinates*, 2nd edn. Academic Press, New York.

Perissinotti P. P., Giugovaz-Tropper B. and Uchitel O. D. (2008) L-Type calcium channels are involved in fast endocytosis at the mouse neuromuscular junction. *Eur. J. Neurosci.* **27**, 1333–1344.

Pestronk A., Adams R. N., Cornblath D., Kuncl R. W., Drachman D. B. and Clawson L. (1989) Patterns of serum IgM antibodies to GM1 and GD1a gangliosides in amyotrophic lateral sclerosis. *Ann. Neurol.* **25**, 98–102.

Piedras-Renteria E. S., Pyle J. L., Diehn M., Glickfeld L. L., Harata N. C., Cao Y., Kavalali E. T., Brown P. O. and Tsien R. W. (2004) Presynaptic homeostasis at CNS nerve terminals compensates for lack of a key Ca^{2+} entry pathway. *Proc. Natl Acad. Sci. USA* **101**, 3609–3614.

Protti D. A., Szczupak L., Scornik F. S. and Uchitel O. D. (1991) Effect of omega-conotoxin GVIA on neurotransmitter release at the mouse neuromuscular junction. *Brain Res.* **557**, 336–339.

Pullen A. H. and Humphreys P. (2000) Ultrastructural analysis of spinal motoneurones from mice treated with IgG from ALS patients, healthy individuals, or disease controls. *J. Neurol. Sci.* **180**(1-2), 35–45.

Rosato Siri M. D. and Uchitel O. D. (1999) Calcium channels coupled to neurotransmitter release at neonatal rat neuromuscular junctions. *J. Physiol.* **514**, 533–540.

Rothstein J. D., Martin L. J. and Kuncl R. W. (1992) Decreased glutamate transport by the brain and spinal cord in amyotrophic lateral sclerosis. *N. Engl. J. Med.* **326**, 1464–1468.

Rowland L. P. (1998) Diagnosis of amyotrophic lateral sclerosis. *J. Neurol. Sci.* **160**, S6–S24.

Schmidt E. R. E., Pasterkamp R. J. and van den Berg L. H. (2009) Axon guidance proteins: novel therapeutic targets for ALS? *Prog. Neurobiol.* **88**, 286–301.

Smaili S., Hirata H., Ureshino R. *et al.* (2009) Calcium and cell death signaling in neurodegeneration and aging. *An. Acad. Bras. Cienc.* **81**(3), 467–475.

Smith R. G., Hamilton S., Hoffman F., Schneider T., Nastainczyk W. and Birnbaumer L. (1992) Serum antibodies to L-type calcium channels in patients with amyotrophic lateral sclerosis. *N. Engl. J. Med.* **327**, 1721–1728.

Smith R. G., Alexianu M. E., Crawford G., Nyormoi O., Stefani E. and Appel S. H. (1994) Cytotoxicity of immunoglobulins from amyotrophic lateral sclerosis patients on a hybrid motoneuron cell line. *Proc. Natl Acad. Sci. USA* **91**, 3393–3397.

Starr T. V. B., Prystay W. and Snutch T. P. (1991) Primary structure of a calcium channel that is highly expressed in the rat cerebellum. *Proc. Natl Acad. Sci. USA* **88**, 5621–5625.

Stea A., Tomlinson W. J., Soong T. W., Bourinet E., Dubel S. J., Vincent S. R. and Snutch T. P. (1994) The localization and functional properties of a rat brain α1A calcium channel reflect similarities to neuronal Q- and P-type channels. *Proc. Natl Acad. Sci. USA* **91**, 10576–10580.

Sutton K. G., McRory J. E., Guthrie H., Murphy T. H. and Snutch T. P. (1999) P/Q-type calcium channels mediate the activity-dependent feedback of syntaxin-1A. *Nature* **401**, 800–804.

Takamori M., Takahashi M., Yasukawa Y., Iwasa K., Nemoto Y., Suenaga A., Nagataki S. and Nakamura T. (1995) Antibodies to recombinant synaptotagmin and calcium channel subtypes in Lambert-Eaton myasthenic syndrome. *J. Neurol. Sci.* **133**(1-2), 95–101.

Troost D., Van Den Ord J. J. and Vianney De Jong J. M. (1990) Immunohistochemical characterization of the inflammatory infiltrate in amyotrophic lateral sclerosis. *Neuropathol. Appl. Neurobiol.* **16**, 401–410.

Uchitel O. D., Appel S. H., Crawford F. and Sczcupak L. (1988) Immunoglobulins from amyotrophic lateral sclerosis patients enhance spontaneous transmitter release from motor-nerve terminals. *Proc. Natl Acad. Sci. USA* **85**, 7371–7374.

Uchitel O. D., Protti D. A., Sanchez V., Cherksey B. D., Sugimori M. and Llinas R. (1992a) P-type voltage-dependent calcium channel mediates presynaptic calcium influx and transmitter release in mammalian synapses. *Proc. Natl Acad. Sci. USA* **89**, 3330–3333.

Uchitel O. D., Scornik F., Protti D. A., Fumberg C. G., Alvarez V. and Appel S. H. (1992b) Long-term neuromuscular dysfunction produced by passive transfer of amyotrophic lateral sclerosis immunoglobulins. *Neurology* **42**, 2175–2180.

Urbano F. J. and Uchitel O. D. (1999) L-type calcium channels unmasked by cell-permeant Ca^{2+}-buffer at mouse motor nerve terminals. *Pflugers Arch.* **437**, 523–528.

Urbano F. J., Piedras-Rentería E. S., Jun K., Shin H. S., Uchitel O. D. and Tsien R. W. (2003) Altered properties of quantal neurotransmitter release at endplates of mice lacking P/Q-type Ca^{2+} channels. *Proc. Natl Acad. Sci. USA* **100**, 3491–3496.

Valdmanis P. N., Daoud H., Dion P. A. and Rouleau G. A. (2009) Recent advances in the genetics of amyotrophic lateral sclerosis. *Curr. Neurol. Neurosci. Rep.* **9**, 198–205.

Van Den Bosch L., Van Damme P., Bogaert E. and Robberecht W. (2006) The role of excitotoxicity in the pathogenesis of amyotrophic lateral sclerosis. *Biochim. Biophys. Acta* **1762**, 1068–1082.

Werz M. A., Elmslie K. S. and Jones S. W. (1993) Phosphorylation enhances inactivation of N-type calcium channel current in bullfrog sympathetic neurons. *Pflugers Arch.* **424**(5-6), 538–545.

Xu Z., Cook L. C., Griffin J. W. and Cleveland D. W. (1993) Increased expression of new filament subunit NF-1 produces morphological alterations that resemble the pathology of human motor neuron disease. *Cell* **73**, 23–33.

Xu L., Guo Y. S., Liu Y. L., Wu S. Y., Yang C., Wu D. X., Wu H. R., Zhang Y. S. and Li C. Y. (2009) Oxidative stress in immune-mediated motoneuron destruction. *Brain Res.* **1302**, 225–232.